Available online at www.sciencedirect.com
ScienceDirect
Polymer 48 (2007) 4021–4027
polymer
www.elsevier.com/locate/polymer

Electrochemical synthesis of functional polypyrrole nanotubes via a self-assembly process

Xiaoming Yang [a,b], Tingyang Dai [a], Zhengxi Zhu [a,1], Yun Lu [a,*]

[a] *Department of Polymer Science and Engineering, State Key Laboratory of Coordination Chemistry, School of Chemistry and Chemical Engineering, Nanjing University, Nanjing 210093, PR China*
[b] *College of Materials Science and Engineering, Soochow University, Suzhou 215123, PR China*

Received 12 January 2007; received in revised form 17 April 2007; accepted 9 May 2007
Available online 18 May 2007

Abstract

We successfully electrochemically polymerized functional polypyrrole (PPy) nanotubes via a self-assembly process in the presence of methyl orange (MO). The influence of polymerization conditions, such as working electrodes and electrochemical polymerization time, on the tubular morphology was discussed. A fibrillar precipitate of MO formed via electric flocculation on the electrode in a neutral aqueous solution prior to the polymerization of pyrrole and acted as a template for the subsequent growth of PPy nanotube. The importance of the MO aggregation in the forming process of PPy nanotubes was revealed by the observation that no tubular structure of PPy formed in dilute MO aqueous solution. The PPy–MO nanotubes obtained showed a high conductivity and an ability to alter photochemically the electrical behavior. In addition, as-prepared PPy tubes could be converted to the corresponding carbonized tubes when they were subjected to thermal treatment under an inert atmosphere.

Keywords: Polypyrrole nanotube; Electrochemical polymerization; Self-assembly

1. Introduction

In the recent past, major advances have been made in the synthesis and characterization of versatile nanostructural materials. These materials continuously attract considerable interest due to their unusual properties and promising potential applications in optics, electronics, and biodiagnostics [1,2]. For such practical uses, conductive polymers with nanostructure, such as nanotubes or nanofibers, may be one of the most notable candidates. Conductive polymers have been extensively explored during the last several decades because of their excellent chemical and physical properties originating from their unique π-conjugated system and switchable conductivity between insulator and metal [3]. In particular, polypyrrole (PPy) has attracted wide attention owing to its good conductivity, redox properties, environmental stability and hitherto a large variety of applications [4]. In addition, PPy can be readily prepared as a film or powder by both electrochemical and chemical approaches in various organic solvents and in aqueous solution.

Conductive polymer nanotubes and nanowires with diameters less than 100 nm can be normally made by hard-template-guided synthesis within the channels, holes, cavities or related nanosized structural units of a template [2a,5]. In this case, post-synthetic treatment is needed to remove the template from the final product in order to recover the nanostructured conductive polymers. Adding structural directing molecules such as surfactants, organic dopants with surfactant functionalities or polyelectrolytes to the chemical polymerization bath is another way to obtain conductive polymer nanostructures [6,7]. Compared with the hard-template-guided synthesis, this soft-template-guided synthesis is simple and cheap, because the cumbersome procedure of fabricating and removing hard templates is not required.

* Corresponding author. Tel.: +86 25 83686423; fax: +86 25 83317761.
E-mail address: yunlu@nju.edu.cn (Y. Lu).
[1] Present address: Department of Chemical Engineering and Materials Science, University of Minnesota, Minneapolis, MN 55455, USA.

0032-3861/$ - see front matter © 2007 Elsevier Ltd. All rights reserved.
doi:10.1016/j.polymer.2007.05.023

Like chemical polymerization, electrochemical synthesis is also a very frequently used technique for obtaining conductive polymers. Many aspects of electrochemical synthesis of conducting polymer nanostructures have been reviewed recently [8]. Most of the works in the field have been done using template- or molecular template-assisted electrosynthesis.

In our previous study, we have reported a new chemical approach, in which a fibrillar complex of anionic azo dye MO (methyl orange, sodium 4-[4′-(dimethyl-amino)-phenyldiazo]phenylsulfonate, $(CH_3)_2NC_6H_4N{=}NC_6H_4SO_3Na$) and oxidant $FeCl_3$ was used as a reactive self-degradable seed template directing the growth of PPy on its surface and promoting the assembly into hollow nanotubular structures [9]. Herein, we further developed the direct electrochemical synthesis of PPy nanotubes on a variety of electrodes in the presence of MO via a self-assembly process. The influence of polymerization conditions, such as working electrodes and electrochemical polymerization time, on the tubular morphology was systematically investigated. The chemical structures of the obtained nanotubes were characterized by Raman, FT-IR and UV–vis. The photoelectrochemical conversional behavior, room-temperature conductivity and thermal stability of the PPy–MO nanotubes were studied by cyclic voltammetry, conductance measurement and TGA. The formation mechanism of the nanotubes was discussed in detail. In addition, carbon nanotubes were fabricated by thermally treating the polymer nanotubes in an inert atmosphere.

2. Experimental section

The pyrrole (Aldrich) monomer was distilled under reduced pressure. Methyl orange (Tianjing Chemical Company, China) was used as received.

Electrochemical polymerizations and cyclic voltammetric measurements were performed in a one-compartment cell with three electrodes at room temperature by using EG&G Model 273 Potentiostat/Galvanostat under the control of a computer. In electrochemical polymerizations, three different plates, i.e. stainless steel, gold and ITO (indium doped tin oxide), were used as the working electrodes. Stainless steel plate was used as a counter electrode and an Ag/AgCl (1 M KCl) electrode was used as the reference electrode. A typical synthesis of the nanotubes was as follows: 105 μL (1.5 mM) pyrrole monomer and 0.0758 g KNO_3 (0.75 mM) (as supporting electrolyte dielectrics) were dissolved in 30 mL of 5 mM methyl orange solution in the cell with stirring. Then constant current density of 1 mA/cm^2 was applied between the working and the counter electrodes. Consequently, a black film of PPy–MO was coated on the working electrode. The obtained film was washed with deionized water/acetone several times and dried under a vacuum atmosphere for 24 h.

In the carbonization procedure, as-prepared PPy–MO films were peeled off from the electrodes and ground to powders. The collected powders were placed in a quartz tube, and heated to 1000 °C at a heating rate of 10 °C min^{-1} under Ar gas flow (0.2 L min^{-1}). After 3 h of carbonization, the quartz tube was naturally cooled to room temperature.

The morphologies were measured by scanning electron microscopy (SEM, JSM-6300, Kevex-Sigma) and transmission electron microscopy (TEM, JEM-200CX). The conductivities were measured by using the standard four-probe method at room temperature. The molecular structure of PPy–MO was characterized by Bruker Vector-22 FT-IR spectrometer and labRAM HR800 (France, Jobin Yvon) Raman spectrometer (excitation wavelength: 532 nm). UV–vis absorption spectra of PPy–MO in *m*-cresol solution were recorded on a UV-240 spectrometer (Shimadzu, Japan). Raman spectra were recorded with a labRAM HR800 (France, Jobin Yvon) using 532 nm laser as the excitation source. An SDT 2960 thermogravimetric analyzer was used to investigate the thermal stability of the PPy–MO with air as pure gas at a flow rate of 50 mL min^{-1}. The heating rate was 10 °C min^{-1}.

3. Result and discussion

3.1. Morphologies observation and analysis

Figs. 1 and 2 show the SEM micrographs of PPy grains and PPy tubules electrochemically synthesized on stainless steel working electrode without and with the addition of MO. The TEM image (Fig. 2A, inset, right) and the electron diffraction patterns (Fig. 2A, inset, left) illustrated that in the initial stages

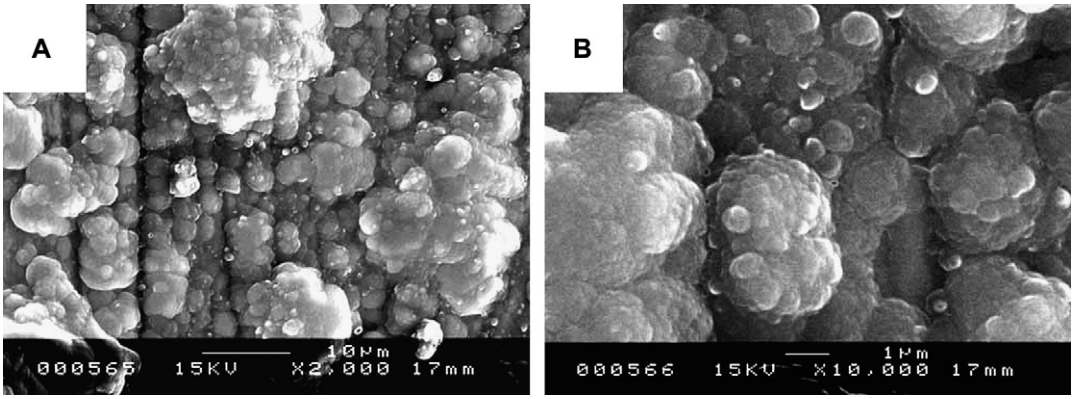

Fig. 1. (A) SEM images of PPy electrochemically synthesized for 30 min (stainless steel electrode, KNO_3); (B) magnified image of (A).

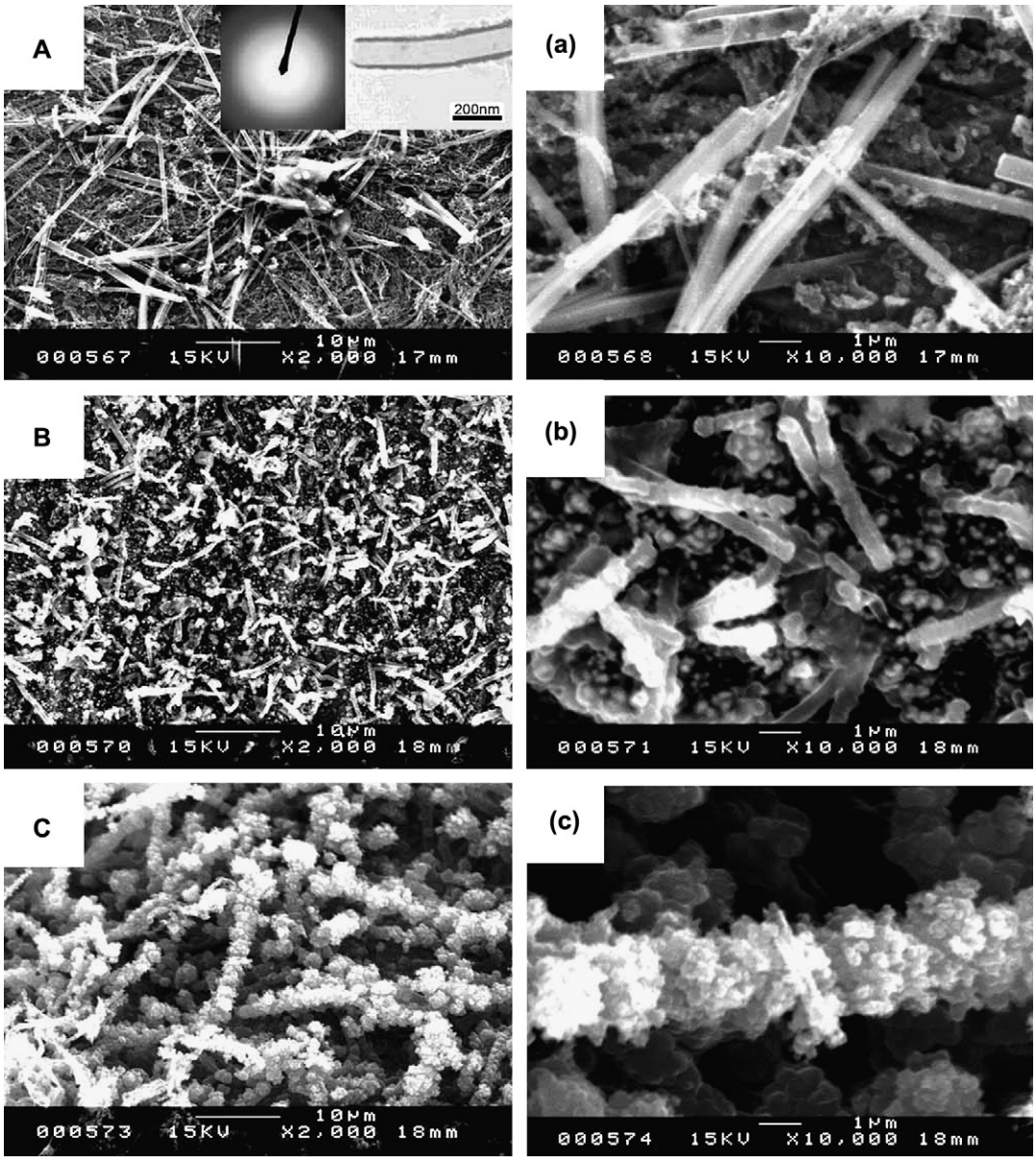

Fig. 2. SEM images of PPy electrochemically synthesized for different times on stainless steel electrode in the presence of MO (5 mM) and KNO_3. (A) 5 min; (B) 20 min; (C) 30 min. (a)–(c) are the magnified images corresponding to (A)–(C), respectively. Insets in (A): right, TEM image of (A); left, electron diffraction image of (A).

of polymerization, the products resulted in the presence of MO are amorphous hollow tubular structure with an inner and outer diameters of 100 and 140 nm, respectively. The self-assembly process of PPy nanotubes doped with naphthaline sulfonic acid (NAS) had been investigated by Wan et al., and the formation mechanism of the tubular morphology was attributed to the surfactant dopant, which also acts as a template [7]. However, in the case of MO, it is not a surfactant molecule since it lacks surfactant properties such as effective lowering of the surface tension and a well-defined critical micelle concentration [10]. Nevertheless, in aqueous solution at 25 °C, MO could dimerize at concentration of 1 mM and form higher oligomers between concentration of 5 and 10 mM [11]. But there is no aggregation in dilute MO aqueous solution. Moreover, MO may form vesicles in combination with an oppositely charged substance [12]. It was found from experimental results that under the concentration of 0.1 mM of MO, formed PPy samples did not give the morphology of nanotubes (results not shown here). Further investigation indicated that, when the concentration of MO was increased to 5 mM, PPy nanotubes appeared on the working electrode surface in initial polymerization time (Fig. 2A and a).

According to previous study, when MO aqueous solution with a concentration of 5 mM was adjusted to acidity, a flocculent precipitate appeared immediately since H^+ promotes the formation of intramolecular salts [13]. In the process of electrochemical polymerization, because of the electrolysis of water and H^+ formed near the surface of the working electrode (anode), it is possible that MO aggregations flocculated around the electrode. In the case of stainless steel electrode, the

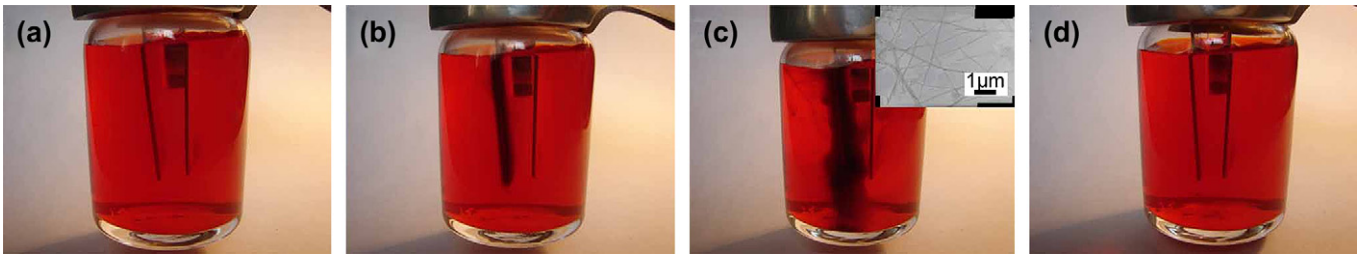

Fig. 3. Electric flocculation process of MO: (a) the initial aqueous solution of MO; the electric current was lasted for (b) 3 min; (c) 10 min (inset: TEM image of the precipitate formed in (c); (d) 10 min after the electric current was cut off. Other conditions: the concentrations of MO and KNO_3 were 5 and 0.75 mM, respectively; stainless steel plates were used as both the working electrode and the counter electrode, and an Ag/AgCl (1 M KCl) electrode was used as the reference electrode.

positive charged Fe^{2+} and $Fe(OH)_2$ were also dissolved from working electrode and these species could as well act as the flocculant [9], which suppressed the electrostatic repulsions between MO aggregations, then destabilized the charged particles and built an amorphous precipitate (Fig. 3). Fortunately, the precipitate had a fibrillar nanostructure (Fig. 3c, inset) and could be redissolved in the neutral aqueous solution in a short time (Fig. 3d). These two features made the precipitate an excellent template for constructing tubular nanostructures [14]. Pyrrole monomers were polymerized preferentially just about on the surface of the fibrillar seed species because the sulfonic groups in MO molecules played a role of active sites for the growth of PPy [15]. It is such species that directed the formation of PPy nanotubular structures.

With the increase of time, the diameter and length of tubules were basically steady, but their surfaces were getting rough (see Fig. 2B and 2b). About 30 min later, grains covered all the outer surface of tubules (as shown in Fig. 2C and 2c), which could be explained by the absence of the aggregation of MO for PPy covered stainless steel working electrode. In the electrochemical polymerization, the optimal polymerization time to get smooth PPy–MO tubules was limited to 10 min.

For our studied system, no template was treated in advance on stainless steel electrode. Thus, the polymerization should belong to the electrochemical templateless polymerization. However, MO self-assembled aggregation formed in the reaction process can themselves act as templates of nanodimensions, and direct the electrochemical polymerization of

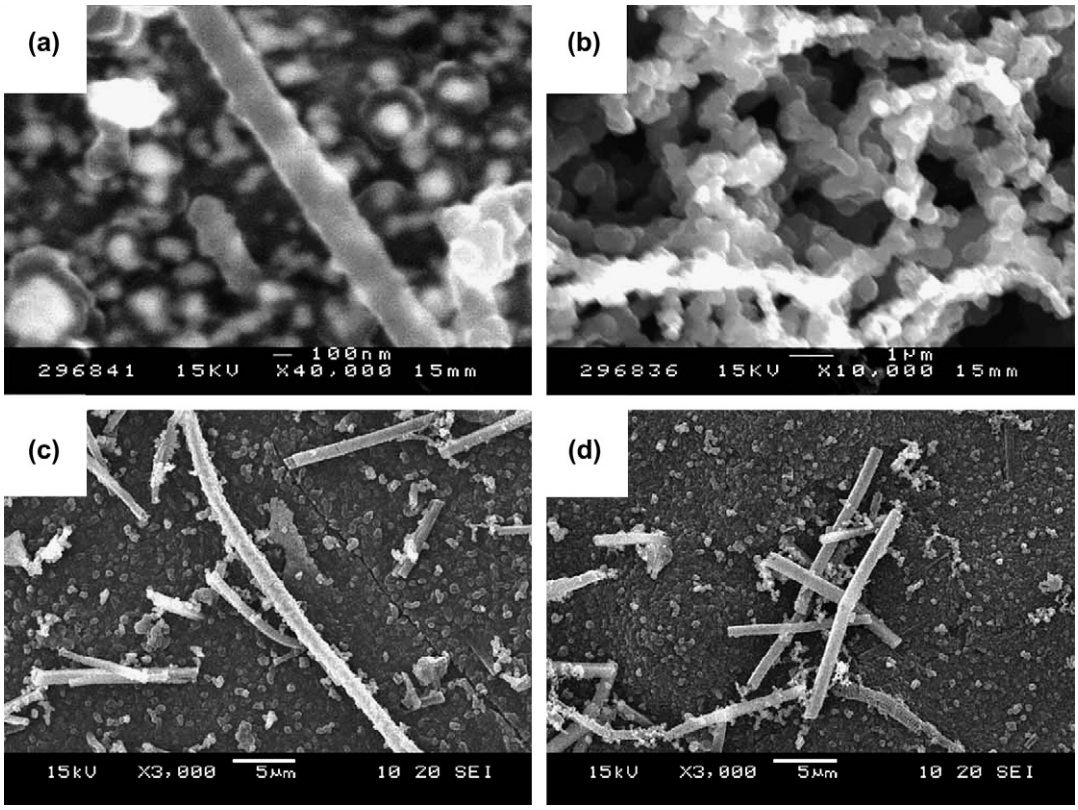

Fig. 4. SEM images of PPy electrochemically synthesized for different times in the presence of MO (5 mM) and KNO_3. (a) 5 min on Au electrode; (b) 30 min on Au electrode; (c) 5 min on ITO electrode; (d) 30 min on ITO electrode.

pyrrole to proceed in a template-like manner. In other words, the stainless steel electrode surface is actually specifically modified with the fibrillar MO self-assembled aggregation when a potential was put on the electrode. So our system could be ascribed to molecular template-assisted one as well.

In electrochemical polymerization, the kind and surface character of electrode applied have an important effect on the actualizing of reaction. In order to study the influence of the electrodes on the tubular morphology of PPy–MO, the gold electrode and ITO electrode were applied as the working electrodes, respectively. It was found that the morphologies of PPy–MO resulted from gold and ITO electrode surfaces (Fig. 4) were obviously different from that obtained from the stainless steel electrode surface. Both tubular and granular PPys were formed on gold electrode and ITO electrode, and the quality of PPy tubes was correspondingly poor.

Such phenomena may be related to the aggregation degree of MO self-assembly on gold or ITO electrode. For both the electrodes, there was only H^+ formed near the anode, and thus much less flocculations of MO appeared on the surface of the inert electrodes under the electric field, compared to stainless steel electrode, around which positive charged Fe^{2+} and $Fe(OH)_2$ as well as H^+ existed. The weaker the flocculability of MO on the electrode surface, the more difficult the formation of PPy nanotubes. Hence, less tubular structures of PPy were obtained on gold or ITO electrode and the quality of formed tubes was also somewhat poor.

3.2. Structural characterization and properties

Raman spectra of PPy–MO tubules and PPy grains electrochemically synthesized on the surface of the stainless steel are shown in Fig. 5. The broader Raman peaks of PPy appearing in the ranges 1000–1150 and 1300–1410 cm^{-1} were assigned to C–H in-plane deformation and ring stretching, respectively. The peak at 1600 cm^{-1} was assigned to C=C backbone stretching of PPy [16]. The characteristic peaks of MO also appeared in the Raman spectra [17], revealing the presence of MO in PPy tubules.

The UV–vis absorption of PPy separately doped with methyl orange (Fig. 6a) and KNO_3 (Fig. 6b) was also studied. Besides the characteristic bands of PPy such as the π–π* absorption at about 400 nm and the bipolaronic absorption at about 560 nm [18], an absorption peak at 430 nm, attributed to the n–π* transition of the *trans*-azobenzene units [19], also appeared in the UV–vis spectrum of the PPy–MO. This result confirmed again the presence of the dopant methyl orange. In order to investigate the photoelectrochemical conversion, cyclic voltammograms of the PPy–MO film were measured upon UV irradiation ($l = 365$ nm, after the first cycle) (see Fig. 7). Without UV radiation, no peaks were

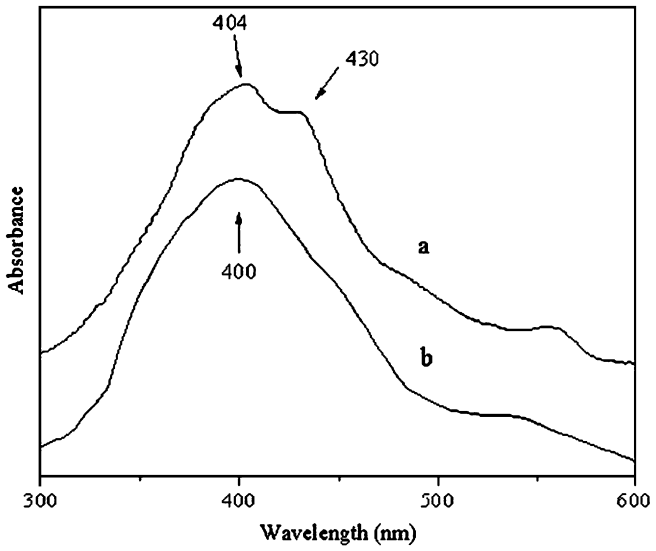

Fig. 6. UV–vis spectra of PPy in *m*-cresol solution, synthesized (a) in the presence of MO as the dopant; (b) in the absence of MO as the dopant.

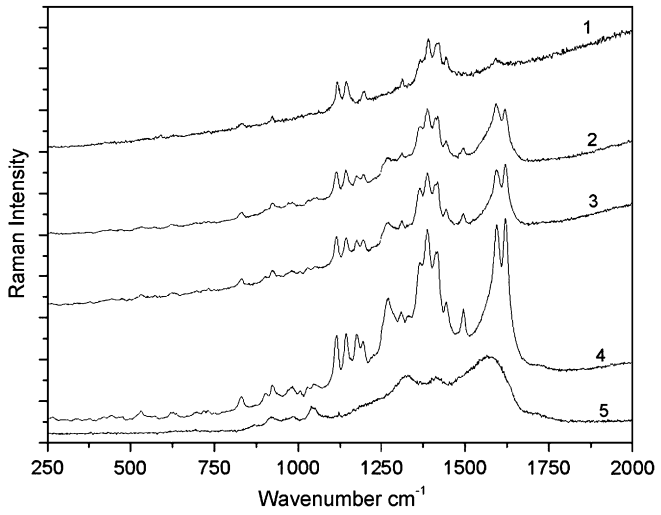

Fig. 5. Raman spectra of MO (1) and PPy electrochemically synthesized for different times in the presence of MO: (2) 10 min; (3) 20 min; (4) 30 min; (5) Raman spectrum of PPy electrochemically synthesized without MO.

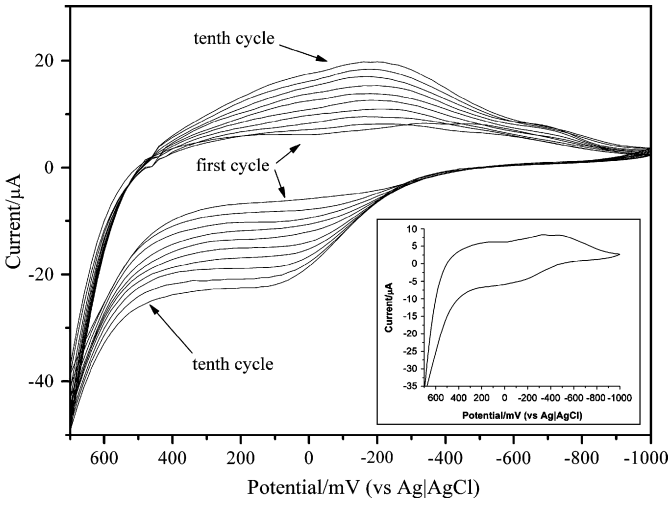

Fig. 7. Cyclic voltammograms of MO-doped PPy film in 0.025 mol/L KNO_3 solution upon UV irradiation ($l = 365$ nm, after the first cycle). Inset: cyclic voltammograms of MO-doped PPy film in 0.025 mol/L KNO_3 solution without UV irradiation. Scan rate: 20 mV/s.

presented at −0.3 and 0.1 V (Fig. 7, inset), due to the fact that all azobenzene units were in the *trans*-state [20]. Once the film was irradiated, the *trans*-azobenzene units were isomerized to the *cis*-state ones, and two peaks were obtained from the reduction of *cis*-state to the hydrazobenzene derivative (HABD, −NH−NH−) at about −0.3 V followed by the oxidation of the HABD at about 0.1 V [20]. With the increase of UV-irradiating time, the peak intensities showed an increase. All these cyclic voltammetric behaviors of the PPy−MO film just agreed with previous reports on the photoelectrochemical conversion of azo compounds [20].

The thermogravimetric analysis indicated that the decomposition temperature of the PPy−MO tubules was only a little higher (about 10 °C) than that of the granules (272 °C) formed from PPy−KNO_3 (Fig. 8). This result could be interpreted by the amorphous structures of these tubules displayed by both TEM electron diffraction patterns (Fig. 2A, inset, left) and XRD data (not shown here). Furthermore, the amorphous structures of PPy−MO tubules suggested that no remarkable improvement on spatial order of polypyrrole arose and methyl orange acted as both a template via self-assembly and a dopant.

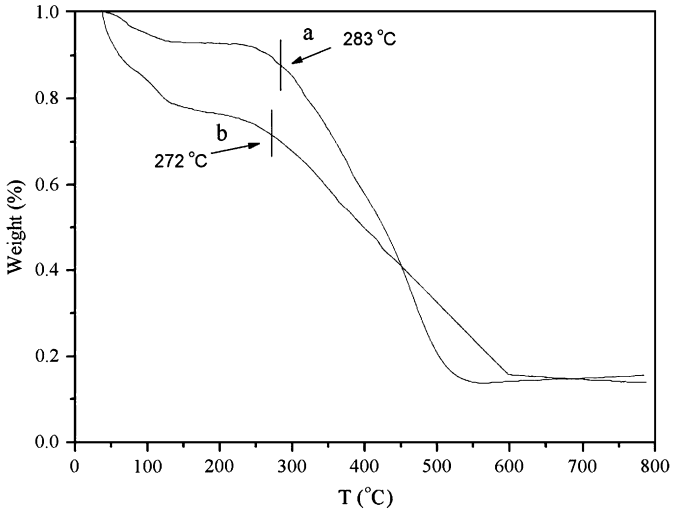

Fig. 8. TGA spectra of PPy electrochemically synthesized (a) in the presence of MO; (b) in the absence of MO.

At room temperature, the conductivity of the PPy−MO tubule film synthesized by electrochemical polymerization was 76 S/cm. This value was higher than that of grain film (8.2 S/cm) doped only with KNO_3 at the same polymerization conditions. From the EDS data, it was found that the degree of doping of the tubule film, [MO]/[Py] ratio (denoted by the ratio $4[S]/([C]-14[S]) = 0.47$), was higher than that of the grain film, $[KNO_3]$/[Py] ratio (denoted by the ratio $([N]-[C]/4)/([C]/4) = 0.35$). Because there was no remarkable enhancement on spatial order of polypyrrole by introducing MO, such a high degree of doping should contribute to the improvement of the conductivity.

3.3. Carbonization of the products

We ground the PPy−MO tubule film to powder, and subjected it to thermal treatment at 1000 °C for 3 h to convert the PPy tubes into corresponding carbon nanotubes. It was earlier reported by Jang and Oh that PPy could be carbonized thermally in an inert atmosphere at elevated temperatures [21]. Fig. 9a shows TEM micrographs of the carbon nanotubes thus obtained. The wall thickness of the carbon nanotube is about 15 nm, which is thinner than that (20 nm) of the original PPy nanotubes. Such a reduction in wall thickness after carbonization appears to be general, which can be ascribed to the formation of more compact structures accompanied by dehydrogenation, denitrogenation and aromatization [22]. According to EDS analysis, the PPy nanotubes carbonized at 1000 °C were composed of C (86.87%), N (3.86%), O (7.74%), S (1.29%) and Cl (0.24%). In the carbonization process of a doped PPy, the loss of nitrogen occurs between 400 and 600 °C, and polycondensed graphitic species are generated [22]. The carbon nanotubes had an average length of ca. micrometers with a broad distribution. The diminution in the length mainly arose from the fracture during the experimental procedure.

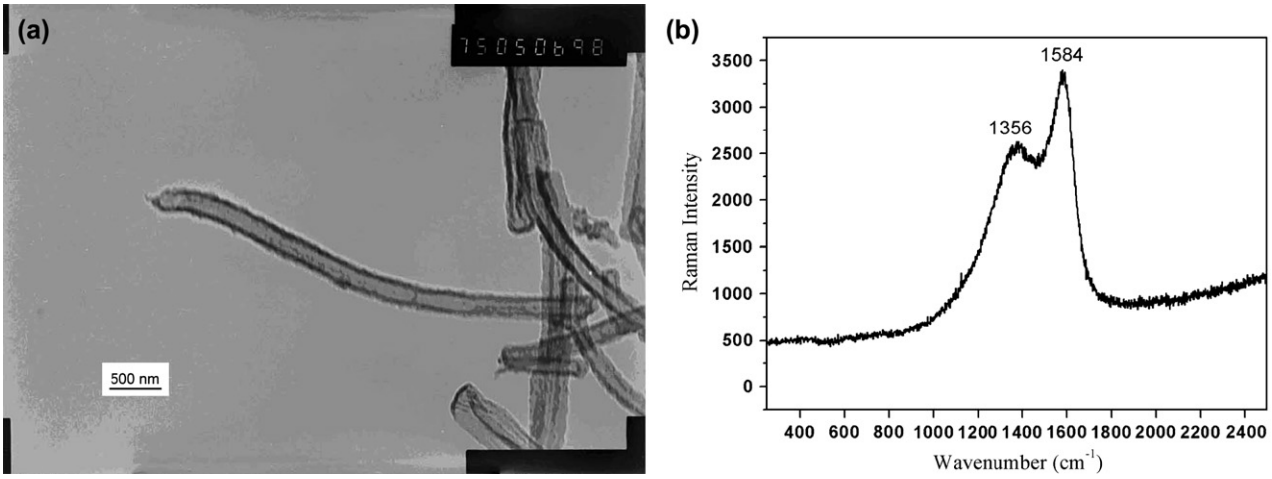

Fig. 9. (a) TEM image of carbon nanotubes obtained from PPy−MO nanotubes after heating for 3 h at 1000 °C. (b) Raman spectrum of as-prepared carbon nanotubes.

Fig. 9b represents the Raman spectra of the carbonized PPy nanotubes. The band at 1584 cm^{-1} (G band) is assigned to the E_{2g} vibration of graphitic carbon with an sp^2 electronic configuration. On the other hand, the peak at 1356 cm^{-1} (D band) is attributable to the A_{1g} mode of diamond-like carbon with an sp^3 configuration. The relative intensity (I_D/I_G) is 0.78, indicating a semicrystalline carbon structure containing some lattice edges or phase defects within the analyzed carbon nanotube [23].

4. Conclusions

We successfully synthesized polypyrrole nanotubes on stainless steel electrode by the direct electrochemical approach in the presence of MO via a self-assembly process. The fibrillar template of MO was formed by electric flocculation on the electrode in a neutral aqueous solution and could be facilely redissolved in a short time when the electric current was cut off. These features made it an outstanding candidate to be used to construct nanotubular structures and remarkably enlarged its practicability. What is more, the azo dye MO also played the dual functions of the dopant and photoelectrochemical conversional substance. The PPy–MO nanotubes obtained showed a high conductivity and an ability to alter the electrical behavior photochemically. By combining the capability of photoelectrochemical conversion of methyl orange and the conductivity of the polypyrrole medium, the resulting new functional material is of potential application for the high-density reversible photoelectrical information storage media, optical switching, electro-optic modulation and so on. They also could be converted into carbonized products by thermally treating them in an inert atmosphere.

Acknowledgement

The authors are grateful for the supports from the National Natural Science Foundation of China (No. 20574034) and Testing Foundation of Nanjing University.

References

[1] Iijima S. Nature 1991;354:56.
[2] (a) Martin CR. Acc Chem Res 1995;28:61;
(b) Dai LM. Smart Mater Struct 2002;11:645;
(c) Yu SF, Lee SB, Martin CR. Anal Chem 2003;75:1239;
(d) Dai LM, Patil A, Gong XY, Guo ZX, Liu LQ, Liu Y, et al. ChemPhysChem 2003;4:1150;
(e) Sapp SA, Mitchell DT, Martin CR. Chem Mater 1999;11:1183;
(f) Zhang GQ, Lu XL, Zhang T, Qu JF, Wang W, Li XG, et al. Nanotechnology 2006;17:4252;
(g) Yui T, Mori Y, Tsuchino T, Itoh T, Hattori T, Fukushima Y, et al. Chem Mater 2005;17:206.
[3] (a) Shirakawa H. Angew Chem Int Ed 2001;40:2575;
(b) MacDiarmid AG. Angew Chem Int Ed 2001;40:2581;
(c) Heeger AJ. Angew Chem Int Ed 2001;40:2591;
(d) Li GF, Martinez C, Semancik S. J Am Chem Soc 2005;127:4903.
[4] (a) Yan F, Xue G, Wan F. J Mater Chem 2002;12:2606;
(b) Li L, Yan F, Xue G. J Appl Polym Sci 2004;91:303;
(c) Zhang XY, Manohar SK. J Am Chem Soc 2005;127:14156.
[5] (a) Wu CG, Bein T. Science 1994;264:1757;
(b) Martin CR. Science 1994;266:1961;
(c) Nicewarner-Pena SR, Freeman RG, Reiss BD, He L, Pena DJ, Walton ID, et al. Science 2001;294:137;
(d) Hermsdorf N, Stamm M, Forster S. Langmuir 2005;21:11987.
[6] Cai ZH, Martin CR. J Am Chem Soc 1989;111:4138.
[7] (a) Yang YS, Wan MX. J Mater Chem 2001;11:2022;
(b) Liu J, Wan MX. J Polym Sci Part A Polym Chem 2001;39:997.
[8] Malinauskas A, Malinauskiene J, Ramanavicius A. Nanotechnology 2005;16:R51–62.
[9] Yang XM, Zhu ZX, Dai TY, Lu Y. Macromol Rapid Commun 2005;26:1736.
[10] Reeves RL, Harkaway SA. J Colloid Interface Sci 1978;64:342.
[11] (a) Quadrifoglio F, Crescenzi V. J Colloid Interface Sci 1971;35:447;
(b) Kendrick KL, Gilkerson WR. J Solution Chem 1987;16:257.
[12] Rixt TB, Jessica MJ, Jan BFNE. Langmuir 1999;15:1083.
[13] Dai TY, Lu Y. Macromol Rapid Commun 2007;28:629.
[14] Dai TY, Yang XM, Lu Y. Nanotechnology 2006;17:3028.
[15] Yassar A, Roncali J, Garnier F. Polym Commun 1987;28:103.
[16] Furukawa Y, Tazawa S, Fujii Y, Harada I. Synth Met 1988;24:329.
[17] (a) Machida K, Lee H. J Raman Spectrosc 1980;9:198;
(b) Machida K, Kim BK, Saito Y, Igarashi K, Uno T. Bull Chem Soc Jpn 1974;47:78.
[18] Bredas JL, Scott JC, Yakushi K, Street GB. Phys Rev B 1984;30:1023.
[19] (a) Huang K, Wan MX. Chem Mater 2002;14:3486;
(b) Tamai N, Miyasaka H. Chem Rev 2000;100:1875;
(c) Kumar GS, Neckers DC. Chem Rev 1989;89:1915.
[20] (a) Liu ZF, Hashimoto K, Fujishima A. Nature 1990;347:658;
(b) Liu ZF, Morigaki K, Enomoto K, Hashimoto K, Fujishima A. J Phys Chem 1992;96:1875.
[21] Jang J, Oh JH. Chem Commun 2004;7:882.
[22] Ando E, Onodera S, Iino M, Ito O. Carbon 2001;39:101.
[23] Tuinstra F, Koenig JL. J Chem Phys 1970;53:1126.